Channel Learning and Communication-Aware Motion Planning in Mobile Networks

Alireza Ghaffarkhah and Yasamin Mostofi

***Abstract*— In this paper we propose a communication-aware motion planning framework to ensure robust cooperative operation of a mobile network in realistic communication environments. We use a probabilistic multi-scale model for channel characterization. We then utilize our previously proposed model-based channel prediction framework in order to devise communication-aware motion-planning approaches. We first propose a motion generation strategy that optimally plans the trajectory of the robot in order to improve its channel learning in an environment. We then propose a communication-aware navigation approach in which link quality predictions are combined with sensing goals in order to ensure cooperative and networked task accomplishment. Our simulation results show the superior performance of our proposed communication-aware motion planning framework.**

I. Introduction

Over the past few years, considerable progress has been made in the area of networked robotic and control systems. The vision of a multi-agent robotic network cooperatively learning and adapting in harsh unknown environments to achieve a common goal is closer than ever. Most of the current research in the robotics and control community, however, assume ideal or over-simplified communication links. For instance, it is common to assume links that are perfect within a certain radius of a node. Such simplified models do not suffice for ensuring robust group operation of a mobile network. Communication plays a key role in the overall performance of robotic networks as the nodes rely on receiving information from others in order to achieve their task. This necessitates considering realistic link models. Furthermore, an integrative approach to communication and control issues is needed, i.e. communication link qualities should be taken into account when motion planning.

The term *communication-aware motion planning* was coined by Y. Mostofi (see [1], [2] for instance) to refer to trajectory generation approaches that take communication link qualities into account. In order to achieve this, each robot should consider the impact of the possible motion decisions on its link qualities when planning its trajectory. This requires each robot to assess the quality of the communication links in the locations that it has not yet visited. As a result, proper prediction of the communication signal strength in a given area, based on only a few measurements, becomes considerably important. In [3], we proposed a framework in which each robot can predict the channel quality based on a small number of measurements, by using probabilistic models [4] to represent the channel. In this paper, we show how our channel prediction framework can be used for building communication-aware motion planning strategies. In particular, we consider two cases. In the first case, we show how the nodes can optimize their trajectory in order to improve their channel prediction quality. In the second case, we show how predictions of the link quality can be combined with other high-level sensing and navigation goals (such as target tracking, obstacle avoidance, etc) in order to ensure robust cooperative operation.

The rest of the paper is organized as follows. In Section II, we describe our system model and briefly summarize the probabilistic multi-scale modeling of a channel. We furthermore show how it can be used for predicting the spatial variations of a wireless link. In section III, we propose communication-aware motion-planning strategies for both channel learning improvement and cooperative task accomplishment. We conclude in Section IV.

II. Wireless Channel Prediction with a Small Number of Measurements

Let $\mathcal{W} \subset \mathbb{R}^2$ denote a workspace, which is possibly punctured by several obstacles. Let $\mathcal{O} \subset \mathbb{R}^2$ denote the union of the obstacle regions. The free configuration space is then given by the set $\mathcal{W}_f = \mathcal{W} - \mathcal{O}$. Consider a mobile node that is operating in this workspace. We assume a point robot with the following dynamics: $q(t+1) = \Psi(q(t), u(t))$, where $q(t) \in \mathcal{W}_f$ is the position of the robot at time t, $u(t) \in \mathcal{U}$ is the control input at time t and $\Psi(.,.)$ is a smooth function. The node needs to maintain its connectivity to a fixed base station while accomplishing its task. In this section, we show how the node can predict its link quality to the base station. More specifically, we provide an overview of our proposed framework for channel learning and prediction based on a very small number of measurements [3], [4]. In the next section, we then propose a communication-aware motion planning framework that optimizes the trajectory of the robot for robust cooperative task accomplishment.

A. Probabilistic Modeling of a Wireless Channel

A fundamental parameter that characterizes the performance of a communication channel is the received Signal to Noise Ratio (SNR), defined as the ratio of the received signal power divided by the receiver thermal noise power. In the wireless communication literature [4], [5], it is well established that the received SNR between two nodes can

This work is supported in part by ARO CTA MAST project # W911NF-08-2-0004 and NSF award # 0812338.

A. Ghaffarkhah and Y. Mostofi are with the Cooperative Network Lab, Department of Electrical and Computer Engineering, University of New Mexico, Albuquerque, NM 87113, USA {alinem, ymostofi}@ece.unm.edu

be modeled as a multi-scale dynamical system with three major dynamics: *Multipath fading (or small-scale fading)*, *Shadowing* and *Path loss*. Fig. 1 shows the received signal power across a route in the basement of the ECE building at UNM. The three main dynamics of the received signal power are marked on the figure. Path loss is the slowest dynamic which is associated with the signal attenuation due to the distance-dependent power fall-off. Depending on the environment, blocking objects might result in a faster variation of the received SNR, referred to as shadowing. Finally, multiple replicas of the transmitted signal can arrive at the receiver due to the reflection from the surrounding objects, resulting in even a faster variation in the received SNR called multipath fading.

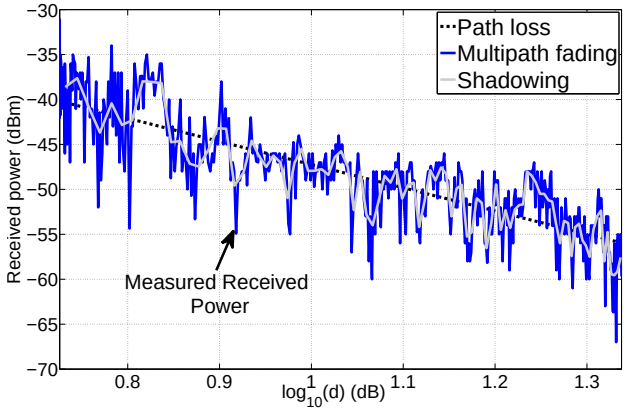

Fig. 1. Underlying dynamics of the received signal power across a route in the basement of the ECE building [3]. d is the distance to the transmitter.

The probabilistic channel modeling framework characterizes the distribution of a sample of the channel as well as its spatial correlation. Here, we briefly summarize this approach [3], [4]. Let $\Upsilon(q)$ denote the received SNR in the transmission from a fixed base station at $q_b \in \mathcal{W}_f$ to a mobile node at $q \in \mathcal{W}_f$. We can characterize $\Upsilon(q)$ by a 2D non-stationary random field with the following form [5]: $\Upsilon(q) = \Upsilon_{\text{mp}}(q)\Upsilon_{\text{sh}}(q)\Upsilon_{\text{pl}}(q)$, where $\Upsilon_{\text{mp}}(q)$ and $\Upsilon_{\text{sh}}(q)$ are random variables representing the multipath fading and shadowing coefficients respectively and $\Upsilon_{\text{pl}}(q) = \frac{K_{\text{pl}}}{\|q-q_b\|^{n_{\text{pl}}}}$ is the distance-dependent path loss. In this model, the multipath fading coefficient, $\Upsilon_{\text{mp}}(q)$, has a unit average. In the communication literature, the distributions of $\Upsilon_{\text{mp}}(q)$ and $\Upsilon_{\text{sh}}(q)$ are established based on empirical data. For instance Nakagami distribution has been shown to be a good match for the distribution of $\Upsilon_{\text{mp}}(q)$ [5]. As for the shadowing variable, $\Upsilon_{\text{sh}}(q)$ is typically modeled by a log-normally distributed random variable. Let $\Upsilon_{\text{dB}}(q) = 10\log_{10}\big(\Upsilon(q)\big)$ represent the received SNR in dB. We have

$$\Upsilon_{\text{dB}}(q) = \underbrace{10\log_{10}\big(K_{\text{pl}}\big) + 10\,\mathbb{E}\Big\{\log_{10}\big(\Upsilon_{\text{mp}}(q)\big)\Big\}}_{K_{\text{dB}}} \\ -10n_{\text{pl}}\log_{10}\big(\|q-q_b\|\big) + \xi(q) + \omega(q) \quad (1)$$

where $\xi(q) = 10\log_{10}\big(\Upsilon_{\text{sh}}(q)\big)$ is a zero-mean Gaussian random variable representing the shadowing effect in dB, $10\,\mathbb{E}\Big\{\log_{10}\big(\Upsilon_{\text{mp}}(q)\big)\Big\}$ is the average of the multipath fading component in dB and $\omega(q) = 10\log_{10}\big(\Upsilon_{\text{mp}}(q)\big) - 10\,\mathbb{E}\Big\{\log_{10}\big(\Upsilon_{\text{mp}}(q)\big)\Big\}$ is a zero-mean random variable, independent from $\xi(q)$, which denotes the impact of multipath fading in dB (after removing its average). Characterizing the spatial correlations of $\xi(q)$ and $\omega(q)$ is also considerably important for our model-based channel prediction framework. As for the spatial correlation of multipath fading, there is no single model that can be a good match for different environments.[1] If the distance between the spatial samples are large enough, the multipath fading component can be considered uncorrelated. This is the assumption we make throughout our derivations in this paper, due to the lack of a better general model. The spatial correlation of shadowing is typically modeled with an exponential function [7]:

$$\mathbb{E}\big\{\xi(q_1)\xi(q_2)\big\} = \rho\big(\|q_1-q_2\|\big) = \alpha e^{-\frac{\|q_1-q_2\|}{\beta}},\ q_1, q_2 \in \mathcal{W}_f, \quad (2)$$

where α is the variance of $\xi(q)$. β is the *decorrelation distance* as it controls how correlated the channel is spatially. In the wireless communication literature, the value of β is reported between 10 m and 50 m for outdoor environments [5]. A typical range for α, on the other hand, is between 4 dB and 13 dB [5].

B. Model-Based Prediction of the Spatial Variations of a Wireless Channel

Consider a case where one or a number of mobile agents want to predict the spatial variations of a wireless channel (in reception from a fixed station), by using only a small number of measurements. Next, we briefly summarize our proposed probabilistic model-based channel prediction framework [3]. In this approach, we only use models for shadowing and path loss terms, due to the lack of a good general model for characterizing the correlation of multipath fading. As such, we take $\omega(q)$ to be a zero-mean spatially uncorrelated noise. The uncorrelated assumption is valid if the spatial samples are far enough in the space.

Consider the case where channel measurements are taken at positions $q_1, \cdots, q_k$. These measurements could be gathered by a robot along its trajectory or cooperatively by a number of robots. Let $Y_k = [y_1, \cdots, y_k]^T \in \mathbb{R}^k$ be the vector of all the available channel measurements in dB. We have

$$Y_k = \underbrace{\begin{bmatrix} 1 & -10\log_{10}(\|q_1 - q_b\|) \\ \vdots & \vdots \\ 1 & -10\log_{10}(\|q_k - q_b\|) \end{bmatrix}}_{H_k} \theta + \Xi_k + \Omega_k, \quad (3)$$

where $\theta = [K_{\text{dB}} \quad n_{\text{pl}}]^T$ is the vector of the path loss parameters, $\Xi_k = [\xi(q_1), \cdots, \xi(q_k)]^T$ and $\Omega_k =$

[1] If the environment is rich in scatterers, for instance, the Fourier transform of the auto-correlation function of multipath fading will have a form that is referred to as Jakes spectrum [6].

$[\omega(q_1), \cdots, \omega(q_k)]^T$. Based on the lognormal model for shadowing, Ξ_k is a zero-mean Gaussian random vector with the covariance matrix $R_k \in \mathbb{R}^{k\times k}$, where $\big[R_k\big]_{i,j} = \rho\big(\|q_i - q_j\|\big)$ for $1 \le i, j \le k$. The term Ω_k denotes the impact of multipath fading. In this paper, we neglect Ω_k when predicting the channel but will consider its effect on the prediction quality. In the following, we first consider the estimation of parameters α, β and θ, based on the available measurements. We then proceed by predicting the channel using the estimated values of path loss and shadowing parameters.

Let $\hat{\alpha}_k$, $\hat{\beta}_k$ and $\hat{\theta}_k$ denote the estimated values of α, β and θ based on k available measurements. Let $\hat{R}_k$ denote the corresponding estimation of R_k, where α and β are replaced by $\hat{\alpha}_k$ and $\hat{\beta}_k$ respectively. Also define R'_k as $R'_k = \hat{R}_k/\hat{\alpha}_k$. We have the following Maximum Likelihood estimation of parameters θ and α [3]:

$$\begin{aligned}\hat{\theta}_k^{\text{ML}} &= \big(H_k^T R_k'^{-1} H_k\big)^{-1} H_k^T R_k'^{-1} Y_k,\\ \hat{\alpha}_k^{\text{ML}} &= \frac{1}{k}\big(Y_k - H_k\hat{\theta}_k^{\text{ML}}\big)^T R_k'^{-1}\big(Y_k - H_k\hat{\theta}_k^{\text{ML}}\big).\end{aligned} \quad (4)$$

More simplified but less optimum estimators can also be derived for θ and α. For instance, if $\beta \to 0$, the samples become uncorrelated, which results in

$$\begin{aligned}\lim_{\beta\to 0}\hat{\theta}_k^{\text{ML}} &= \underbrace{\big(H_k^T H_k\big)^{-1} H_k^T Y_k}_{\hat{\theta}_k^{\text{uncor}}},\\ \lim_{\beta\to 0}\hat{\alpha}_k^{\text{ML}} &= \underbrace{\frac{1}{k}\big(Y_k - H_k\hat{\theta}_k^{\text{uncor}}\big)^T\big(Y_k - H_k\hat{\theta}_k^{\text{uncor}}\big)}_{\hat{\alpha}_k^{\text{uncor}}}.\end{aligned} \quad (5)$$

Therefore, the estimate of θ and α will not depend on the estimate of β, as expected. Estimation of β, on the other hand, is typically more challenging due to matrix invertibility issues [3]. A robust practical but suboptimum strategy can be devised as follows [3]. Let $\tilde{R}_k$ represent the estimate of R_k through numerical averaging. Then, we can find the β that results in the best exponential fit to $\tilde{R}_k$ (measured by the Frobenius norm of the difference in dB) as follows:

$$\hat{\beta}_k = \frac{1}{|\mathcal{D}_k|}\sum_{d\in\mathcal{D}_k}\frac{d}{\log\big(\hat{\alpha}_k\big) - \log\big(\tilde{\rho}_k(d)\big)}, \quad (6)$$

where $\mathcal{D}_k = \big\{d \;\big|\; \tilde{\rho}_k(d) \le \hat{\alpha}_k\big\}$, $|\mathcal{D}_k|$ denotes the size of set $\mathcal{D}_k$ and $\tilde{\rho}_k(d)$ is the numerical estimate of the correlation function at distance d, based on the available measurements. This can also be extended to a weighted approach as follows: $\hat{\beta}_k = \frac{1}{\sum_{d\in\mathcal{D}_k}\tau(d)}\sum_{d\in\mathcal{D}_k}\frac{\tau(d)d}{\log(\hat{\alpha}_k)-\log(\tilde{\rho}_k(d))}$, where the weight $\tau(d)$ is chosen based on our assessment of the accuracy of the estimation of $\tilde{\rho}_k(d)$. For instance, if we have very few measurements at a specific distance between two points, then the weight should be smaller. If the location of the transmitting node (fixed station) is not known, the path loss parameters can be estimated by finding the best line fit to the log of the received measurements (as can be seen from Fig. 1). Similarly, α can be estimated by calculating the deviation from this average and β can be estimated as explained previously. Alternatively, the position of the base station can also be added to the unknown parameters and jointly estimated.

Once the underlying parameters are estimated, we can estimate the channel, based on the available measurements and at any arbitrary position $q \in \mathcal{W}_f$ as follows:

$$\hat{\Upsilon}_{\text{dB},k}(q) = h^T(q)\hat{\theta}_k + \hat{\phi}_k^T(q)\hat{R}_k^{-1}\big(Y_k - H_k\hat{\theta}_k\big), \quad (7)$$

where $h(q) = \Big[1 \quad -10\log\big(\|q - q_b\|\big)\Big]^T$ and $\hat{\phi}_k(q) = \Big[\hat{\alpha}_k\; e^{-\|q-q_1\|/\hat{\beta}_k}, \cdots, \hat{\alpha}_k\; e^{-\|q-q_k\|/\hat{\beta}_k}\Big]^T$. This linear estimator minimizes the MSE of the estimation error (assuming correct parameters) and is a conditional average of the field.

C. Sensitivity of Channel Prediction to Parameter Estimation Errors

The quality of our channel prediction framework depends on how well we estimate the underlying parameters of the multi-scale model. In this section, we explore the impact of error in parameter estimation on the overall channel estimation performance. We can easily derive the following expression for channel prediction error covariance at position $q \in \mathcal{W}_f$, given the current estimate of the parameters:

$$\begin{aligned}\hat{\sigma}^2_{\text{dB},k}(q) \triangleq \mathbb{E}\Big\{\big(\Upsilon_{\text{dB}}(q) - \hat{\Upsilon}_{\text{dB},k}(q)\big)^2 \;\Big|\; \hat{\alpha}_k, \hat{\beta}_k, \hat{\theta}_k\Big\} =\\ \alpha + \sigma_\omega^2 + \hat{\phi}_k^T(q)\hat{R}_k^{-1}\Big[U_k\hat{R}_k^{-1}\hat{\phi}_k(q) - 2\phi_k(q)\Big] +\\ \Big[h(q) - H_k^T\hat{R}_k^{-1}\hat{\phi}_k(q)\Big]^T\delta\theta_k\,\delta\theta_k^T\Big[h(q) - H_k^T\hat{R}_k^{-1}\hat{\phi}_k(q)\Big],\end{aligned} \quad (8)$$

where $\delta\theta_k = \theta - \hat{\theta}_k$, $\sigma_\omega^2 = \mathbb{E}\{\omega^2(q)\}$, $U_k = R_k + \sigma_\omega^2 I_k$, I_k is the k dimensional identity matrix and $\phi_k(q)$ is the exact version of $\hat{\phi}_k(q)$ (see Eq. 7), defined as $\phi_k(q) = \Big[\alpha\, e^{-\|q-q_1\|/\beta}, \cdots, \alpha\, e^{-\|q-q_k\|/\beta}\Big]^T$. Let the Average Normalized Mean Square Error (ANMSE) of channel prediction be defined as follows: ANMSE $= \frac{\int_{\mathcal{W}_f}\hat{\sigma}^2_{\text{dB},k}(q)dA}{\int_{\mathcal{W}_f}\Upsilon^2_{\text{dB}}(q)dA}$. Fig. 2 shows the impact of parameter estimation uncertainty on the overall channel prediction quality where the NMSE of the channel prediction is averaged over a 10.0 m by 10.0 m rectangle workspace with the origin at the center of the space. The base station is located outside the workspace at $q_b = [20.0 \quad 20.0]^T$ in this case. The channel is simulated using our probabilistic channel simulator with the following parameters: $\alpha = 4.0$, $\beta = 10$ m and $\theta = [-12.89 \;\; 3.0]^T$. In this case, no multipath fading is simulated. The number of available channel measurements is taken to be 0.2% of the total samples (grid size) with the measurements randomly distributed over the workspace. The figure shows the impact of error in parameter estimation on the overall channel prediction performance. For each curve, only one parameter is perturbed while the rest are assumed perfect. It can be seen that the curves attain their minima when there is no parameter estimation error, as expected. We can furthermore observe that uncertainty in the estimation of different parameters impacts the performance differently. As can be seen, the

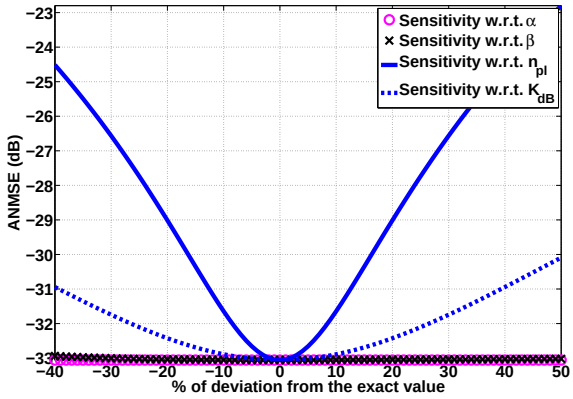

Fig. 2. Average Normalized Mean Square Error (ANMSE), spatially averaged over the workspace, as a function of the % of estimation error in $\hat{\alpha}_k$, $\hat{\beta}_k$ and $\hat{\theta}_k$.

prediction is more sensitive to the path loss parameters (especially the exponent n_{pl}). In other words, the effect of an error in the estimation of the shadowing parameters is negligible, when compared to that of the path loss parameters. Next, we derive an expression for the prediction error covariance at position $q \in \mathcal{W}_f$, given only the current estimate of the shadowing parameters. In this case, path loss parameters are derived by using the estimated shadowing parameters and Eq. 4. We have,

$$\begin{aligned}\sigma^2_{\text{dB},k}(q) \triangleq \mathbb{E}\Big\{\big(\Upsilon_{\text{dB}}(q) - \hat{\Upsilon}_{\text{dB},k}(q)\big)^2 \;\Big|\; \hat{\alpha}_k, \hat{\beta}_k\Big\} = \\ \mathbb{E}\Big\{\Big(- \big[h(q) - H_k^T \hat{R}_k^{-1}\hat{\phi}_k(q)\big]^T M_k\big(\Xi_k + \Omega_k\big) + \\ -\hat{\phi}_k^T(q)\hat{R}_k^{-1}\big(\Xi_k + \Omega_k\big) + \xi(q) + \omega(q)\Big)^2 \;\Big|\; \hat{\alpha}_k, \hat{\beta}_k\Big\} = \\ \alpha + \sigma_\omega^2 + \hat{\phi}_k^T(q)\hat{R}_k^{-1}\Big[U_k\hat{R}_k^{-1}\hat{\phi}_k(q) - 2\phi_k(q)\Big] + \\ \Big[h(q) - H_k^T\hat{R}_k^{-1}\hat{\phi}_k(q)\Big]^T \hat{P}_k^\theta \Big[h(q) - H_k^T\hat{R}_k^{-1}\hat{\phi}_k(q)\Big] + \\ 2\Big[h(q) - H_k^T\hat{R}_k^{-1}\hat{\phi}_k(q)\Big]^T M_k\Big[U_k\hat{R}_k^{-1}\hat{\phi}_k(q) - \phi_k(q)\Big],\end{aligned} \tag{9}$$

where $M_k = \big(H_k^T\hat{R}_k^{-1}H_k\big)^{-1}H_k^T\hat{R}_k^{-1}$ and $\hat{P}_k^\theta = M_k U_k M_k^T$ is the estimation error of the path loss parameters when the erroneous shadowing parameters are used. Note that in the absence of shadowing parameter estimation error and multipath, we have

$$\begin{aligned}\lim_{\substack{\hat{\alpha}_k\to\alpha \\ \hat{\beta}_k\to\beta \\ \sigma_\omega\to 0}} \sigma^2_{\text{dB},k}(q) = \alpha - \phi_k^T(q)R_k^{-1}\phi_k(q) + \\ \Big[h(q) - H_k^T R_k^{-1}\phi_k(q)\Big]^T P_k^\theta \Big[h(q) - H_k^T R_k^{-1}\phi_k(q)\Big],\end{aligned} \tag{10}$$

where $P_k^\theta = \big(H_k^T R_k^{-1} H_k\big)^{-1}$ is the error covariance of path loss estimation in case the shadowing parameters are known. Finally, in the perfect case where both path loss and shadowing parameters are estimated with no error and there is no multipath fading, the channel prediction error covariance is simplified to

$$\lim_{\substack{\hat{\theta}_k\to\theta \\ \hat{\alpha}_k\to\alpha \\ \hat{\beta}_k\to\beta \\ \sigma_\omega\to 0}} \sigma^2_{\text{dB},k}(q) = \alpha - \phi_k^T(q)R_k^{-1}\phi_k(q). \tag{11}$$

III. Communication-Aware Motion Planning

The main purpose of communication-aware motion planning is to utilize the acquired knowledge on the link quality in order to optimally plan the motion, in the presence of communication constraints. There are different ways that our channel prediction framework can be utilized to improve networked performance. In this section, we mainly discuss two possibilities. In the first case, a mobile node wants to learn the spatial variations of the channel (as discussed in the previous section). Since the node samples the channel along its trajectory, its motion directly impacts its channel learning quality. Then, we want to answer the following question "what is the optimum trajectory that provides the best channel prediction quality?". In the second case, the node wants to accomplish a given task, such as target tracking, while maintaining and optimizing its connectivity. We next consider these two cases.

A. Adaptive Communication-Aware Motion Planning for Channel Learning

Consider the case where $k \geq 0$ channel measurements are available to the mobile node at time instant t. Then, the node wants to plan its trajectory such that the next channel measurement it gathers, minimizes its overall channel prediction error covariance of the next step. Note that we consider a discrete-time motion dynamics in this paper, as discussed earlier. Let $\sigma^2_{\text{dB},k+1,\text{ave}}$ denote the spatial average of the channel prediction error covariance when one more measurement is gathered, i.e. total of $k+1$ measurements are available:$\sigma^2_{\text{dB},k+1,\text{ave}} = \frac{\int_{\mathcal{W}_f}\sigma^2_{\text{dB},k+1}(q)dA}{\int_{\mathcal{W}_f}dA}$. Then the next optimum position is the one that, when added to the current available measurements, minimizes $\sigma^2_{\text{dB},k+1,\text{ave}}$. In real-time applications, however, evaluating the prediction error covariance over the whole space at every time step, in order to form this objective, could be computationally prohibitive. Therefore, here we discuss a sub-optimum alternative with a close enough performance. Consider the case where the next position is chosen where $\sigma^2_{\text{dB},k}(q)$ is maximum. In other words, the next position is the one where we have the highest prediction error covariance (entropy) based on our current measurements. Then, we introduce the following objective function

$$J_{\text{chnl},k,t}(u) \triangleq \sigma^2_{\text{dB},k}\big(\Psi(q(t),u)\big), \tag{12}$$

and the following adaptive motion-planning optimization problem:

$$\begin{cases} u^*(t) = \arg\max\; J_{\text{chnl},k,t}(u) \\ \text{s.t. } \Psi(q(t),u) \in \mathcal{W}_f, \;\; u \in \mathcal{U} \end{cases} \tag{13}$$

where $u(t)$ is the control input at time t, $\mathcal{U}$ is the set of admissible control inputs and $\mathcal{W}_f$ is the obstacle-free

navigation area. As for $\sigma^2_{\text{dB},k}(q)$, either Eq. 10 or 11 can be used.

As an example, consider the workspace of Fig. 3, where a fixed station is located at $q_b = [30.0 \quad 30.0]^T$. A mobile node needs to operate in this environment, while maintaining its connectivity to this station. As such, it first wants to optimally plan its motion in order to collect a few channel measurements for channel prediction in the whole workspace. Fig. 3 shows the zero-one spatial map of the received SNR from the fixed base station, where the black areas are the regions where the nodes will lose their connectivity to the base station. The packet dropping threshold is set to $\Upsilon_{\text{dB},T} = -55.00$ dB in this case, i.e. any received packet with SNR below this level is dropped. Note that we showed the zero-one map of the channel in Fig. 3 only for the sake of better visualization i.e. the goal here is to predict the exact map of the received SNR (not the zero-one version). Our channel is a simulated channel with $\theta = [-12.89 \quad 3.0]^T$, $\alpha = 4.0$ and $\beta = 10.0$ m. As for multipath fading, Υ_{mp} is simulated using a Rician-fading distribution [5], which results in the following pdf: $f_{\Upsilon_{\text{mp}}}(\Upsilon) = (1+K_b)e^{-K_b-(1+K_b)\Upsilon} B_0\Big(2\sqrt{\Upsilon K_b(K_b+1)}\Big)$, where $B_0(.)$ is the modified zeroth-order Bessel function and K_b is the Rician K-factor. Note that $K_b = 0$ results in an exponential distribution, which has a considerable amount of channel variations, while $K_b = \infty$ results in no fading, i.e. we will have a channel with only path-loss and shadowing. For the example of Fig. 3, $K_b = 5$ is chosen. The figure shows the sharp variations of the SNR, which makes maintaining connectivity challenging if traditional communication-unaware approaches are used. Fig. 4 shows the trajectory of a mobile agent where the proposed adaptive communication-aware motion planning method of Eq. 13 is used. For the sake of simplicity, we assume a holonomic agent with the following dynamics: $q(t+1) = q(t) + u(t)$, where $u(t) \in \mathcal{U} = \{u \mid \|u\| \leq u_{\max}\}$. The empty circle and the filled one denote the initial and final positions of the node respectively. In this example, the channel is known apriori (at time $t = 0$) at only $1.0\,\%$ of the workspace. Then at every time step, one more channel measurement becomes available. Fig. 5 shows the Average Normalized Mean Square Error (ANMSE) of channel prediction (in dB) as a function of time, where the averaging is done over the whole workspace. Finally, Fig. 6 shows snapshots of the prediction error covariance as a function of position for four different time instants. It can be seen that channel prediction improves considerably with time, as the node intelligently optimizes its motion accordingly.

B. Communication-Aware Motion Planning for Robust Task Accomplishment

In this part, we propose a communication-aware motion planning framework that is aimed at task accomplishment, while maintaining connectivity. Without loss of generality, we discuss the framework in the context of a cooperative target tracking problem. Consider a target-tracking scenario, where a mobile node measures the position of a moving

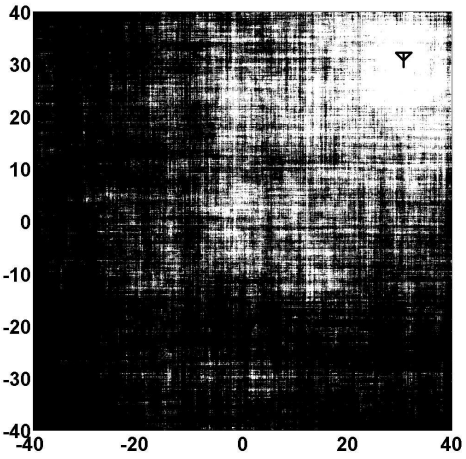

Fig. 3. The zero-one map of the received SNR in the reception from the base station.

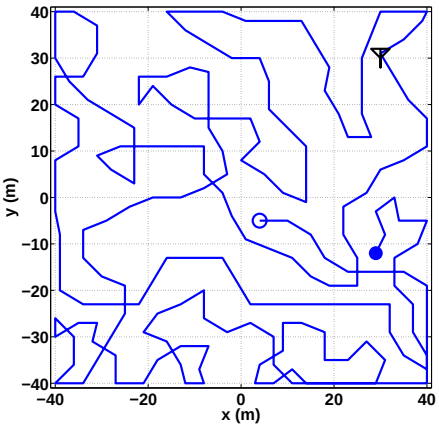

Fig. 4. Adaptive communication-aware motion planning for channel learning and prediction.

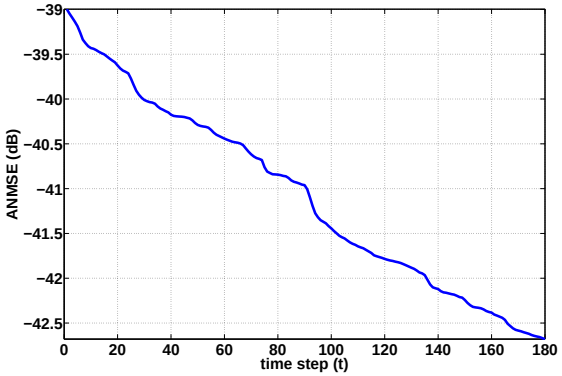

Fig. 5. Spatial Average (over the whole workspace) of the Normalized Mean Square Error (ANMSE) of channel prediction as a function of time.

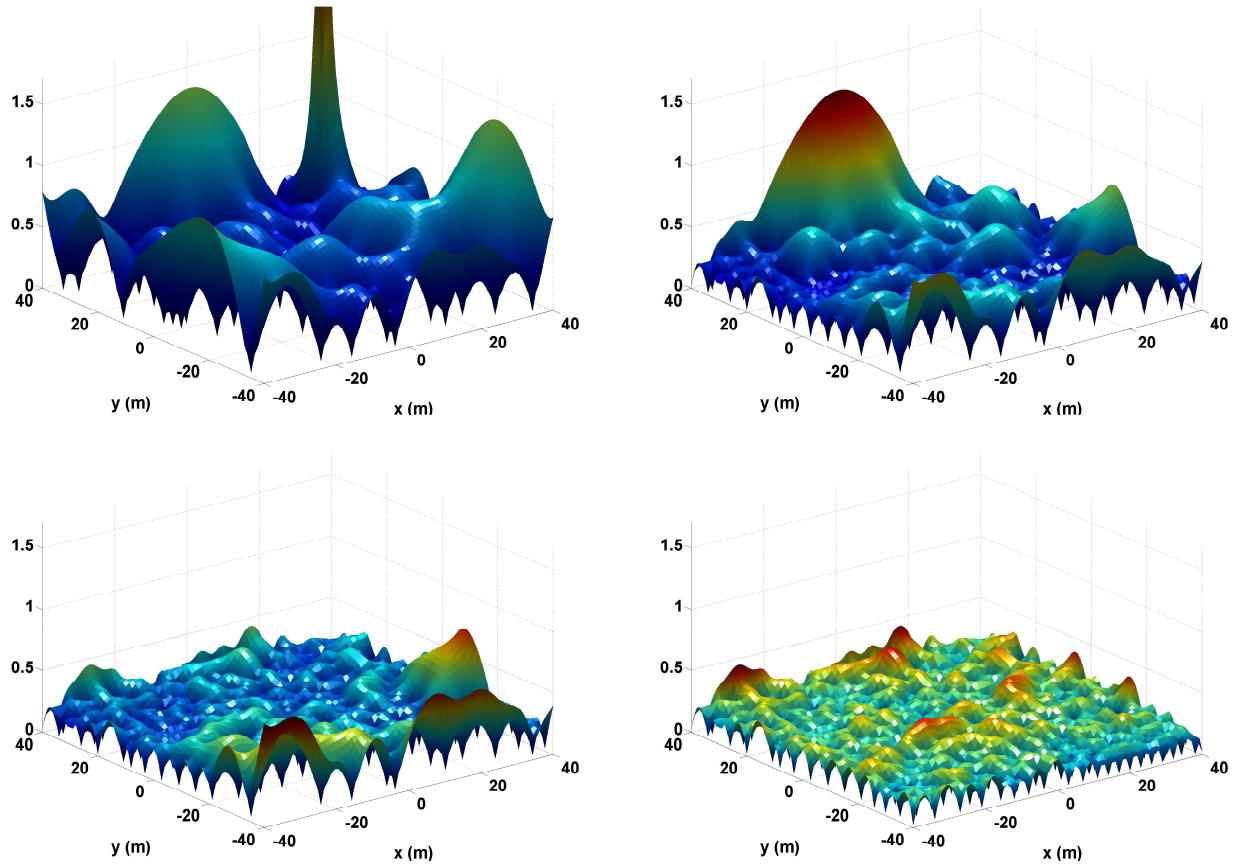

Fig. 6. Snapshots of the prediction error covariance ($\sigma^2_{\mathrm{dB},k}(q)$) in the workspace (top left for $t = 0$, top right for $t = 80$, bottom left for $t = 120$ and bottom right for $t = 200$).

target and sends its measurements to a fixed base station. The overall goal is for the station to constantly have the best assessment of the target position. The communication link between the robot and the base station is a realistic communication channel with path loss, shadowing and multipath fading. In most robotics and navigation literature, only target tracking objectives are considered when motion planning. As such, the robot can lose its connection to the base station several times, resulting in a poor cooperative performance. In this section, we propose a communication-aware motion planning framework that navigates the robot to positions that give the best estimate of target position while trying to maintain the connectivity to the base station. We assume a packet dropping receiver [8], [9] at the base station, i.e. the receiver drops all the erroneous packets. In order to do so, the receiver compares the received SNR with a pre-calculated threshold necessary for an error-free reception. Any packet with the received SNR below this level will be dropped. Let $\Upsilon_{\mathrm{dB},T}$ be the error-free SNR threshold. Then the received packet is dropped at time t if $\Upsilon_{\mathrm{dB}}(q(t)) < \Upsilon_{\mathrm{dB},T}$ and is kept otherwise.

Let $x(t) \in \mathcal{W}$ denote the position of a moving target at time t. We consider the following dynamical model for the moving target: $x(t+1) = Ax(t) + \zeta(t)$, where $\zeta(t) \in \mathbb{R}^2$ is a zero-mean Gaussian noise with $\Theta(t) = \mathbb{E}\{\zeta(t)\zeta^T(t)\}$ representing its covariance matrix. Let $z(t) \in \mathbb{R}^2$ represent the measurement of the mobile node of $x(t)$. We have $z(t) = x(t)+v(t)$, where $v(t) \in \mathbb{R}^2$ is a zero-mean Gaussian observation noise with $\Lambda(t) = \mathbb{E}\{v(t)v^T(t)\}$ representing its covariance. The remote base station estimates the position of the target, based on the received observations, by using a Kalman filter. Let $\hat{x}(t_1|t_2)$ represent the estimate of $x(t_1)$ using all the received observations up to and including time t_2. We assume that the uplink channel (channel from mobile node to the base station) and the downlink one (channel from the base station to the mobile node) have the same quality. This assumption could be valid for a good number of scenarios but not for all cases. For instance, in our example Time Division Duplexing (TDD) can be used as the communication is from the base station to the mobile node in the channel learning phase and vice versa in the task accomplishment phase, resulting in a symmetric uplink and downlink. Thus, in order to indicate the link quality from the mobile node to the base station in this part, we use the same notations that indicated the link quality from the base station to the mobile node in the previous section. Let $P_x(t_1|t_2)$ denote the corresponding estimation error covariance at the base station at time t_1, given $\Upsilon_{\mathrm{dB}}(q(0)), \cdots, \Upsilon_{\mathrm{dB}}(q(t_2))$ for

$t_2 \leq t_1$. Note that Kalman filtering in the presence of packet-dropping links is different from its traditional form since $P_x(t_1|t_2)$ is a stochastic matrix due to its dependency on $\Upsilon_{\text{dB}}(q(0)), \cdots, \Upsilon_{\text{dB}}(q(t_2))$. Define

$$\lambda(t) = \begin{cases} 1 & \Upsilon_{\text{dB}}(q(t)) \geq \Upsilon_{\text{dB},T} \\ 0 & \text{else} \end{cases} \tag{14}$$

Then Kalman filtering over a packet dropping link can be expressed as follows [10]:

$$\begin{aligned} \hat{x}(t+1|t+1) &= A\hat{x}(t|t) + \lambda(t+1)K_f(t+1) \\ &\quad \times \big(z(t+1) - A\hat{x}(t|t)\big) \\ P_x(t+1|t) &= AP_x(t|t)A^T + \Theta(t) \\ K_f(t+1) &= P_x(t+1|t)\Big(P_x(t+1|t) + \Lambda(t+1)\Big)^{-1} \\ P_x(t+1|t+1) &= P_x(t+1|t) \\ &\quad - \lambda(t+1)K_f(t+1)P_x(t+1|t). \end{aligned} \tag{15}$$

By defining the Fisher information matrix as $\mathcal{J}_x(t_1|t_2) = \big(P_x(t_1|t_2)\big)^{-1}$, we have,

$$\begin{aligned} \mathcal{J}_x(t+1|t) &= \Big(A\big(\mathcal{J}_x(t|t)\big)^{-1}A^T + \Theta(t)\Big)^{-1} \\ \mathcal{J}_x(t+1|t+1) &= \mathcal{J}_x(t+1|t) + \underbrace{\lambda(t+1)\Lambda^{-1}(t+1)}_{\mathcal{I}_x(t+1)}. \end{aligned} \tag{16}$$

We refer to $\mathcal{I}_x(t+1)$ as the information innovation at time $t+1$, as it shows the amount of new information that is received at the base station at time $t+1$. Note that $\mathcal{I}_x(t+1)$ depends on both the sensing quality of the mobile node as well as its communication quality to the base station. As can be seen, the information innovation term is stochastic due to its dependency on the link quality. We then propose a communication-aware navigation strategy that aims to maximize the average Fisher information innovation of the next step, using the channel prediction framework of the previous section. We have

$$\begin{aligned} &\mathbb{E}\big\{\mathcal{J}_x(t+1|t+1)\big|\Upsilon_{\text{dB}}(q(0)), \cdots, \Upsilon_{\text{dB}}(q(t))\big\} = \\ &\mathcal{J}_x(t+1|t) + \mathbb{E}\big\{\mathcal{I}_x(t+1)\big\} \end{aligned} \tag{17}$$

and

$$\mathbb{E}\big\{\mathcal{I}_x(t+1)\big\} = \text{Prob}\Big\{\Upsilon_{\text{dB}}(q(t+1)) \geq \Upsilon_{\text{dB},T}\Big\}\Lambda^{-1}(t+1), \tag{18}$$

where the averaging is done over link quality. $\text{Prob}\Big\{\Upsilon_{\text{dB}}(q(t+1)) \geq \Upsilon_{\text{dB},T}\Big\}$ is the probability that the received packet is kept at the base station at time $t+1$. The mobile node can assess this probability by using the channel learning framework of the previous section (note that we assumed the same uplink and downlink). At every time step, the mobile node predicts the channel (over its workspace), based on the available channel measurements. It can then assess the probability of having a connection as follows: $\text{Prob}\Big\{\Upsilon_{\text{dB}}(q(t+1)) \geq \Upsilon_{\text{dB},T}\Big\} \approx Q\left(\frac{\Upsilon_{\text{dB},T} - \hat{\Upsilon}_{\text{dB},k}(q(t+1))}{\sigma_{\text{dB},k}(q(t+1))}\right)$, where $Q(r) = \frac{1}{\sqrt{2\pi}}\int_r^\infty e^{-\tau^2/2}d\tau$ is the Q-function and k is the number of channel measurements available for channel prediction. The approximation sign is used since we derived this expression by neglecting the impact of multipath fading. Let $\mathcal{I}_x(t+1|t)$ denote the predicted information innovation at time $t+1$, based on the observations up to and including time t. We have the following objective function for communication-aware motion planning:

$$\begin{aligned} J_{\text{tgt},k,t}(u) &\triangleq \text{tr}\Big(\mathbb{E}\big\{\mathcal{I}_x(t+1|t)\big\}\Big)\Big|_{\substack{q(t+1)\leftarrow\Psi(q(t),u) \\ x(t+1)\leftarrow\hat{x}(t+1|t)}} \\ &= Q\left(\frac{\Upsilon_{\text{dB},T} - \hat{\Upsilon}_{\text{dB},k}(q(t+1))}{\sigma_{\text{dB},k}(q(t+1))}\right)\text{tr}\big(\Lambda^{-1}(t+1)\big)\Big|_{\substack{q(t+1)\leftarrow\Psi(q(t),u), \\ x(t+1)\leftarrow\hat{x}(t+1|t)}} \end{aligned} \tag{19}$$

where tr(.) denotes the trace, and the following optimization problem:

$$\begin{cases} u^*(t) = \arg\max\ J_{\text{tgt},k,t}(u) \\ \text{s.t. } \Psi(q(t),u) \in \mathcal{W}_f, \ \ u \in \mathcal{U} \end{cases} \tag{20}$$

Fig. 7 shows the trajectory of a mobile agent in a target tracking scenario, when the proposed algorithm is used. The empty circles/boxes and the filled ones denote the initial and final positions respectively. The dynamical model of the mobile agent is the same as in the previous example. The parameters of the simulated channel are as follows: $\theta = [-12.89 \quad 3.0]^T$, $\alpha = 2.0$ and $\beta = 10.0$m, with the packet-dropping threshold set to -55.0 dB. Moreover, we added a Rician fading with $K_b = 5$ to simulate the effect of multipath. As for the sensing model, we assume the distance-dependent model introduced in [11] for the observation noise covariance: $\Lambda(t) = T^T\big(\varphi(t)\big)L(t)T\big(\varphi(t)\big)$, where $L(t) = \begin{bmatrix} g\big(\|q(t)-x(t)\|\big) & 0 \\ 0 & \varrho g\big(\|q(t)-x(t)\|\big) \end{bmatrix}$, $\varphi(t)$ is the angle between the vector $q(t)-x(t)$ and x-axis in a global frame, $g(.)$ is a real positive analytic function representing the range noise variance, $\varrho > 0$ is a scaling constant and T is the 2D rotation matrix. We choose the following quadratic form for g: $g(r) = \eta(r-r_s)^2 + \varepsilon$, where η and ε are positive constants and r_s is the sweet spot radius (sensing quality is the best at this radius). In the example of Fig. 7, we use $\eta = 0.05$, $\varepsilon = 0.01$, $\varrho = 5$ and $r_s = 5$ m.

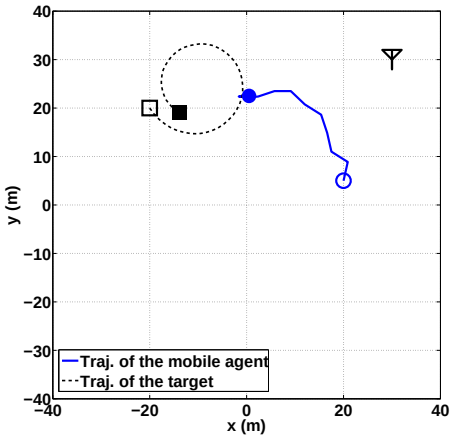

Fig. 7. Communication-aware target tracking based on maximizing the average received information innovation.

Fig. 8 shows $\mathrm{tr}\big(\mathbb{E}\big\{P_x(t|t)\big\}\big)$, the trace of the average estimation error covariance after Kalman filtering at the base station. For comparison, the figure also shows the performance for the communication-unaware case (which considers only the sensing quality). It can be seen that the communication-aware case performs considerably better than the unaware one. For instance, the unaware approach positions the node at the sweet spot radius, which minimizes only the sensing error covariance. On the other hand, the communication-aware approach finds the motion trajectory that results in the best tradeoff between sensing and communication qualities. Finally, Fig. 9 shows the trace of the instantaneous information innovation at the base station, $\mathcal{I}_x(t)$, for one run. It can be seen that the communication-unaware approach loses its connectivity.

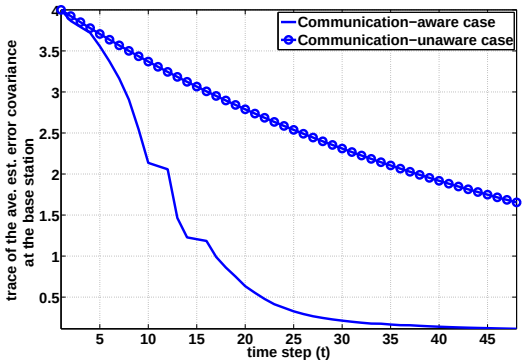

Fig. 8. Trace of the average estimation error covariance (after Kalman filtering and averaged over channel distribution) at the base station for both communication-aware and unaware cases.

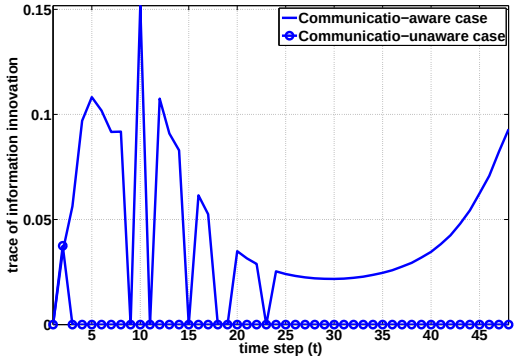

Fig. 9. Trace of the instantaneous information innovation received at the base station for both communication-aware and unaware cases.

C. Combined Channel Learning and Motion Planning for Communication-Aware Coordination of Robotic Networks

The two objective functions, introduced in the previous sections, can be combined to obtain a general time-varying objective function for communication-aware motion planning: $J_{\mathrm{tot},k,t}(u) = J_{\mathrm{tgt},k,t}(u) + \gamma(t)J_{\mathrm{chnl},k,t}(u)$, where $\gamma(t) \geq 0$ can be chosen to have pure channel prediction improvement without task achievement (Section III-A), or pure communication-aware task achievement (Section III-B) or a mixture of the two. The optimal $u(t)$ is then the solution to the following optimization problem:

$$\begin{cases} u^*(t) = \arg\max\ J_{\mathrm{tot},k,t}(u) \\ \text{s.t. } \Psi(q(t),u) \in \mathcal{W}_f, \ \ u \in \mathcal{U} \end{cases} \tag{21}$$

IV. Conclusions

In this paper we proposed a communication-aware motion generation framework to ensure robust cooperative operation in realistic communication environments. We used a probabilistic multi-scale model for channel characterization as well as our previously proposed model-based channel prediction framework, in order to devise communication-aware motion-planning strategies. We considered two cases: motion-planning for channel learning and motion planning for task accomplishment. For the first case, we proposed a motion generation strategy that optimally plans the trajectory of the robot in order to improve its channel learning in an environment. For the second case, we proposed a communication-aware navigation approach in which link quality predictions are combined with sensing goals in order to ensure cooperative task accomplishment. Our simulations results compared the performance with communication-unaware approaches and showed the superior performance of our proposed framework in realistic communication environments.

References

[1] Y. Mostofi. Communication-Aware Motion Planning in Fading Environments. In *Proceedings of IEEE 25th International Conference on Robotics and Automation (ICRA)*, pages 3169–3174, Pasadena, CA, May 2008.

[2] Y. Mostofi. Decentralized communication-aware motion planning in mobile networks: An information-gain approach. *Journal of Intelligent and Robotic Systems, Special Issue on Unmanned Autonomous Vehicles*, 56, 2009.

[3] Y. Mostofi, M. Malmirchegini, and Ghaffarkhah. Estimation of communication signal strength in robotic networks. In *To appear in 2010 IEEE International Conference on Robotics and Automation (ICRA2010)*, 2010.

[4] Y. Mostofi, A. Gonzalez-Ruiz, A. Ghaffarkhah, and D. Li. Characterization and Modeling of Wireless Channels for Networked Robotic and Control Systems - A Comprehensive Overview. In *Proceedings of 2009 IEEE/RSJ International Conference on Intelligent Robots and Systems (IROS)*, St. Louis, MO, October 2009.

[5] A. Goldsmith. *Wireless Communications*. Cambridge University Press, 2005.

[6] W. C. Jakes. *Microwave Mobile Communications*. Wiley-IEEE Press, New York, 1994.

[7] M. Gudmundson. Correlation model for shadow fading in mobile radio systems. *Electronics Letters*, 27(23):2145–2146, Nov. 1991.

[8] A. Ghaffarkhah and Y. Mostofi. Communication-aware navigation functions for cooperative target tracking. In *Proc. of the 2009 American Control Conference*, pages 1316–1322, June 2009.

[9] A. Ghaffarkhah and Y. Mostofi. Communication-aware target tracking using navigation functions - centralized case. In *Proc. of the Second International Conference on Robot Communication and Coordination (ROBOCOMM)*, pages 1–8, March 31 2009-April 2 2009.

[10] Y. Mostofi and R. Murray. To Drop or Not to Drop: Design Principles for Kalman Filtering over Wireless Fading Channels. *IEEE Transactions on Automatic Control*, 54(2):376–381, February 2009.

[11] K. Umeda, J. Ota, and H. Kimura. Fusion of multiple ultrasonic sensor data and imagery data for measuring moving obstacle's motion. In *Intl. Conf. on Multisensor Fusion and Integration for Intelligent Systems*, pages 742–748, December 1996.